Development of proxy model for production forecast using adaptive neuro-fuzzy inference system and experimental design

Akeem Olatunde Arinkoola*,
Ugochukwu I. Duru and
Haruna Monday Onuh

African University of Science and Technology (AUST),
Km 10, Airport Road,
Galadimawa, Abuja, Nigeria
Email: moranroolaakeem@yahoo.com
Email: ugooduru@yahoo.com
Email: onuhharuna@yahoo.com
*Corresponding author

Abstract: Proxy-models are computationally cheap alternative to full numerical simulation during production performance predictions. They are widely use in reservoir management to forecast production in order to assist investment decisions. However, the underperformance of many E&P projects is due to unrealistic forecast quantities arising from assumptions, human biases and reservoir modelling limitations. Hence, considerable efforts are needed to bridge gaps between forecasts and the actual production. The reservoir under study is developed with six producing wells, all deviated. The internal reservoir heterogeneity believed to have created significant fluid flow anisotropy which trapped the remaining mobile oil in the compartments poorly contacted by the current producing well spacing. Consequently, the proposed reservoir management is Infill drilling. This study utilised simulation model for well selection and its optimal placement within the reservoir. Experimental design technique and adaptive neuro-fuzzy inference system (ANFIS) were integrated to develop predictive model for production forecast given new development option. Comparison of the conventional response surface (RSM) and ANFIS models was made based on their prediction performances. The ANFIS model was found to be superior.

Keywords: proxy-model; production forecast; response surface models; RSM; numerical simulation; experimental design; adaptive neuro-fuzzy inference system; ANFIS.

Reference to this paper should be made as follows: Arinkoola, A.O., Duru, U.I. and Onuh, H.M. (2015) 'Development of proxy model for production forecast using adaptive neuro-fuzzy inference system and experimental design', *Int. J. Petroleum Engineering*, Vol. 1, No. 3, pp.189–220.

Biographical notes: Akeem Olatunde Arinkoola is a PhD candidate in the Department of Petroleum Engineering at the African University of Science and Technology, Abuja, Nigeria. His area of interest includes reservoir engineering, uncertainty analysis and reservoir management. He is a Lecturer in the Department of Chemical Engineering, Ladoke Akintola University of Technology (LAUTECH), Ogbomoso, Nigeria.

Ugochukwu I. Duru is a PhD candidate at the African University of Science and Technology, Abuja, Nigeria. His special areas of interests are petroleum production and drilling fluid optimisation. He is a Lecturer in the Department of Petroleum Engineering, Federal University of Technology, Owerri, Nigeria.

Haruna Monday Onuh is a PhD candidate at the African University of Science and Technology, Abuja, Nigeria. He specialises in reservoir characterisation. He is currently a Petroleum Engineer at Halliburton, Lagos, Nigeria.

1 Introduction

The increasing necessity for quantifying uncertainties and their associated effects on investment decisions has become very important in management decisions. This is one of the major reasons why the use of experimental design and associated response surface models (RSM) has been on the increase in the E&P industry. Prior to development of RSM, uncertainty screening is usually performed to reduce number of experimental runs during which some impactful parameters may not be selected for regression process. This result to unrealistic forecast quantity for economic decisions. In order to bridge gaps between the forecasts and the actual production, this study combined experimental design and adaptive neuro-fuzzy inference system (ANFIS) to develop a predictive model for production forecast of a real Niger Delta Field. Experimental design was employed for uncertainty screening and data gathering while ANFIS technique was utilised for predictive model development.

Proxy-models are often used to assist the production optimisation process such as proposing optimal in-fill well locations, type and number (Guyagular et al., 2000; Badru and Kabir, 2003; Ozdogan et al., 2005; Yeten, 2007). RSM-based proxy-models are routinely used as input to a Monte Carlo sampling process (Fishman, 1996) due to possible high exhaustive sampling rates. However, RSM can be a problem if high degree of nonlinearity exists between the input and output variables. The use of artificial neural network (ANN) and Krigging has been reported for resolving nonlinearity issues (Peng and Gupta, 2004). Appropriate selection of experimental design and sampling techniques can significantly improve model predictability (Yeten et al., 2005). Yeten et al. (2005) studied different experimental designs and proxy-models and their capability to predict uncertainties in selected field performance. A good result was reported in application of kriging and splines proxy-models with space filling (*Latin hypercube*) design. But the same types of proxy-models gave worse results for traditional designs (e.g., Placket Burman, central composite and D-optimal designs). The creation of proxy-models of a high quality is therefore related to the selection of appropriate experimental design algorithms, the quality of the input dataset as well as the degree of linearity and nonlinearity of input-output relationship.

ANN according to Mohaghegh (2000) is part of a group of analytic tools that attempts to imitate life to address the problem of input-output relationship. ANN has been presented as an important tool that can be applied to map the response surface in the multidimensional spaces of a reservoir model (Cullick et al., 2006). The mapped response is then used as a substitute of reservoir simulation runs during history matching and production forecast processes. Some limitations of ANN are highlighted by Mohaghegh

(2000) and Olatunji et al. (2011). Recent studies have shown that these limitations can be overcome through the application of another sensitivity-based linear learning methods (SBLLM) in the conventional feed forward neural network (FFNN) and the use of fuzzy logic (Sampaio et al., 2009; Olatunji et al., 2011).

According to Olatunji et al. (2011), SBLLM is an improvement that was able to solve the instability problem. Fuzzy logic as pointed out by Salam et al. (2011), has ability to capture knowledge from data that is inherently imprecise and maintaining a high level of performance in the presence of uncertainty. The original Back-propagation method used in Nets was found to exhibit slow convergence due to large search space dimensions for learning. Fuzzy inference system (FIS) employs hybrid-learning rules for training process.

ANFIS employs hybrid-learning algorithm, which is a combination of gradient descent and the least-squares method. In the forward pass of the hybrid learning algorithm, node outputs would go forward until last layer and the consequent parameters would be identified by the least-squares method (Jang, 1993). In the backward pass, the error signals propagate backwards and the premise parameters would be updated by gradient descent. The consequent parameters are optimised under the condition that the premise parameters are fixed. Thus, hybrid approach converges much faster than conventional backward propagation as applied to ANN. However, in the training step using ANFIS method, the influence clustering radius is usually evaluated by trial-and-error using different membership function. This procedure can be time demanding especially if the degree of nonlinearity between the dependent and independent variables are considerably significant.

2 Brief reservoir model description

The dynamic simulation model was constructed by integrating static model, rock and fluid properties, production data and well completions. A 100 × 100 × 1 ft grid dimension was used to preserve reservoir heterogeneity and accommodate simulation runs. On the average from well log interpretation, the reservoir porosity is 28.4%, water saturation 27% and permeability 700 mD. From fluid characterisation, the initial reservoir pressure, Pi = 1935 psia, the oil gravity is 20.7, oil formation volume factor (FVF) is 1.17, and reservoir average temperature is 165°F. Model initialisation confirmed the estimated stock tank oil originally in place (STOOIP) to be approximately 68 million. This figure agreed to the estimated P50 uncertainty value of 66.8 MMstb with maximum deviation of 1.2 MMstb. The P10 and P90 values recorded from the Monte Carlo simulation are 59.2 MMstb and 75.53 MMstb respectively.

3 Model calibration

Reservoir model was developed by integrating static and dynamic data. This was done in Eclipse data file (see Appendix D). The simulator is a combination of diffusivity equation, transport equation and equation of state. Eclipse utilises a data file (reservoir model) that allows for the integration of data for numerical simulation. Such

model has to be calibrated before any accepted forecast could be made using the model. Model calibration is synonymous to history matching. By history matching it means conditioning the numerical model to the historical data then use the resultant model for production forecast. This was done on both well by well and on field levels using traditional method (Rwechungura et al., 2011) and the objective functions considered include well water-cut for all the wells and pressure (FPR), gas-oil ratio (GOR), water-cut (FWC) and water production (FWPT) at reservoir level. Several parameters were sensitised upon to achieve a good match but the following are the major ones adjusted:

1 Vertical permeability was degraded globally by 15%. This improved the water production in Well-02 by enhancing the lateral flow of water in this area that allowed matching the water cut.

2 Fault transmissibility was increased to match the water-cut in Well-04.

3 Critical water saturation was increased by a factor of 2 to match the water breakthrough time (WBT) in Well-01. The connate water saturations obtained from the static model were relatively low.

Figure 1(a) shows the results of the field-wide history matching and consists of four different graphs of various responses with time on the horizontal axis. The dotted points indicate the observed data while the continuous line the simulated values. The pressure match is shown in black colour, water cut and cumulative water produced in blue and the GOR in red. Figure 1(b) shows the water-cut match for four wells. It is clear that the breakthrough time and observed water-cut levels were matched in all the plots. However, the imperfection in the match of the field WBT correctly was due to the geology and proximity of some wells to oil-water-contact. Nevertheless, the field matching was good and the model was taken as reservoir proxy suitable to use for further analysis.

Figure 2 shows post-history match distribution of the residual oil saturation in some selected layers of the reservoir. It is obvious that beyond the life of the existing wells, substantial residual oil saturation is left behind.

4 Infill well selection and placement

For additional recovery, a number of production schemes were considered using the calibrated model. This includes evaluation of the types and the optimum placement of the infill wells, the use of all vertical wells or all horizontal wells, or a combination of both horizontal and vertical wells. The well placement was optimised for each scheme considered by placing the wells one at a time and running the simulation for 18 years. For the horizontal wells, the evaluation of the vertical placement and optimal lateral length was simulated assuming horizontal length of 700 metres and 1,000 metres as the case usually are in the Niger Delta. The inter-well spacing assumed was 800 metres. In all the simulations, WBT and recoverable oil are the reservoir responses.

Figure 1 (a) Field pressure and saturation match (b) Well saturation match (see online version for colours)

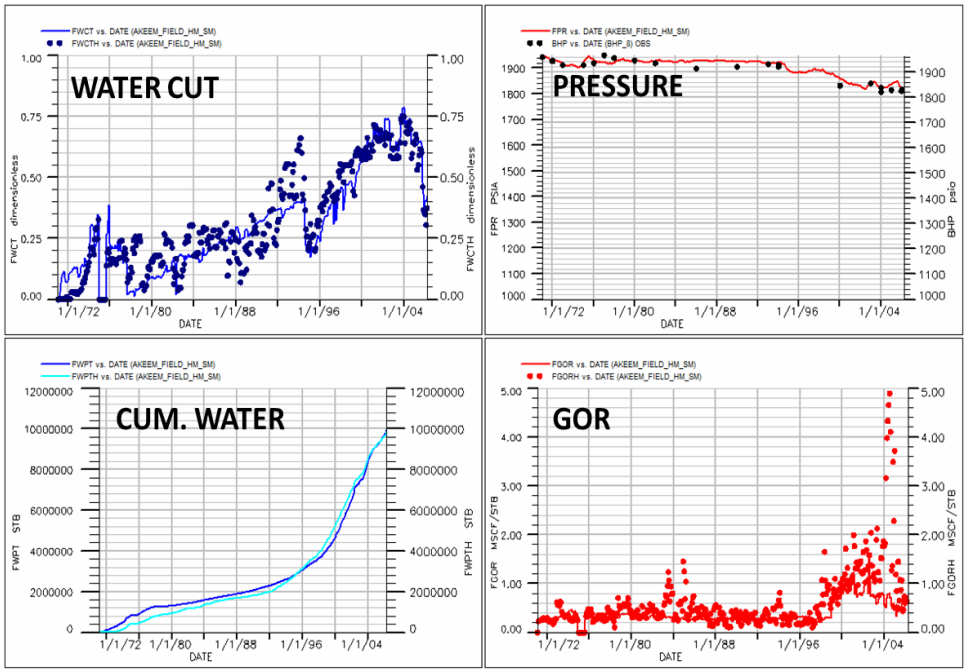

(a)

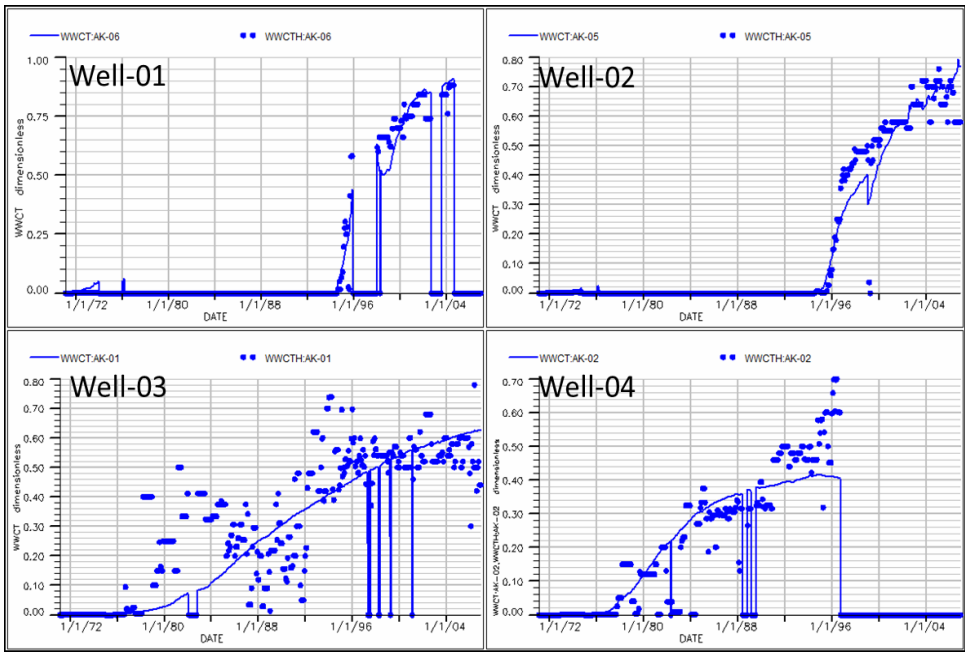

(b)

Figure 2 Distribution of the residual oil saturation at the end of history match in some layers of the reservoir (see online version for colours)

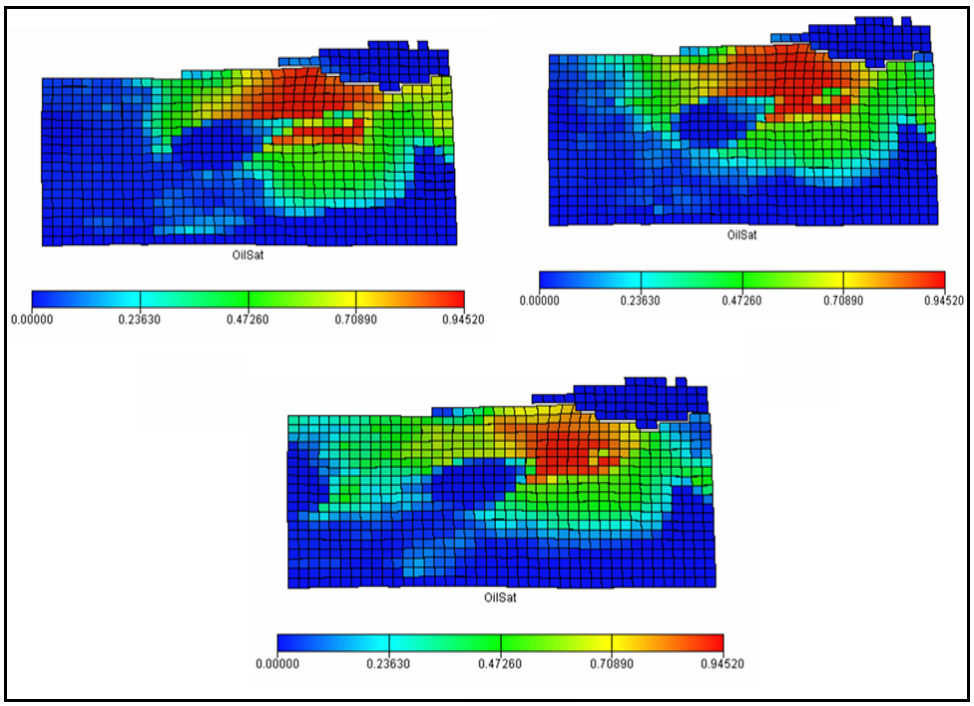

The reservoir was divided into four different sub-regions using faults. In all these regions, permeability ranges from 100 mD to 1,300 mD and porosities range between 10% and 27%. Porosity and permeability histograms for all the regions are displayed in Figures B1 and B2 in Appendix B. It is clearly observed that the geology of the different sub-region is different. Both the porosity and permeability distributions agreed geologically with high permeability found mostly in high porosity regions.

Table 1 shows the result of the simulation. The table compares the performance of the horizontal and vertical wells across the reservoir sub-regions as well as the effects of the lateral length of the horizontal wells on production and water break through time. The recommendations to drill or not was based strictly on number of wells, WBT and cumulative oil recovery. The results show that in all the recommended regions for infill drilling horizontal wells with 1,000 m lateral lengths gave higher productivity.

Drilling two horizontal wells each of lateral length of 700 metres in Region 1 produced 5 MMSTB the same quantity obtained from drilling four vertical wells in the same region. This region can be said to be almost depleted or homogeneous because the simulation result indicated no significant difference in additional reserves by using 1,000 metres and 700 metres horizontal well lengths. Considering additional reserves, a horizontal well is optimum with well length of 700 metres in Region 1 and Region 3. However, it was observed that all wells (vertical and horizontal) experienced WBT one month after production hence, infill drilling in Region 1 and Region 3 was not a viable option. Drilling two horizontal wells each with lateral length of 1,000 metres in Region 2 and Region 4 allows more recovery and exhibited delay in WBT.

Table 1 Summary of Wells performance for optimum well selection and placement

Reservoir	*Well type*	*No. of wells*	*Well length (m)*	*Cum. oil (MMSTB)*	*WBT (days)*	*Remark*
Region 1	Vertical	4	NA	5	30	
	Horizontal	2	700	5	30	No infill
			1,000	5.3	30	
Region 2	Vertical	4	NA	5.5	549	
	Horizontal	2	700	5.3	1,491	Infill
			1,000	6	1,614	
Region 3	Vertical	4	NA	6.2	30	
	Horizontal	2	700	6.2	30	No Infill
			1,000	6.5	30	
Region 4	Vertical	4	NA	7	30	
	Horizontal	2	700	6	519	Infill
			1,000	7	641	

Note: NA – not applicable

As shown in Figure 3, a better performance was obtained with four horizontal wells compared to eight vertical wells. For optimal number of infill well required, three horizontal wells were drilled and simulated. First, two completed in Region 2 and one in Region 4. Then, with one horizontal well completed in Region 2 and two horizontal wells drilled and completed in Region 4. A significant difference in additional reserve was produced with four horizontal wells when compared with the three horizontal wells. Based on this analysis, a total of four horizontal wells were drilled. The recoverable hydrocarbon simulated was 31.84 MMstb as shown in Figure 3. This value corresponds to a recovery factor of 46.8%.

Figure 3 Comparison of incremental production from vertical and horizontal wells with four horizontal wells outperformed eight vertical wells (see online version for colours)

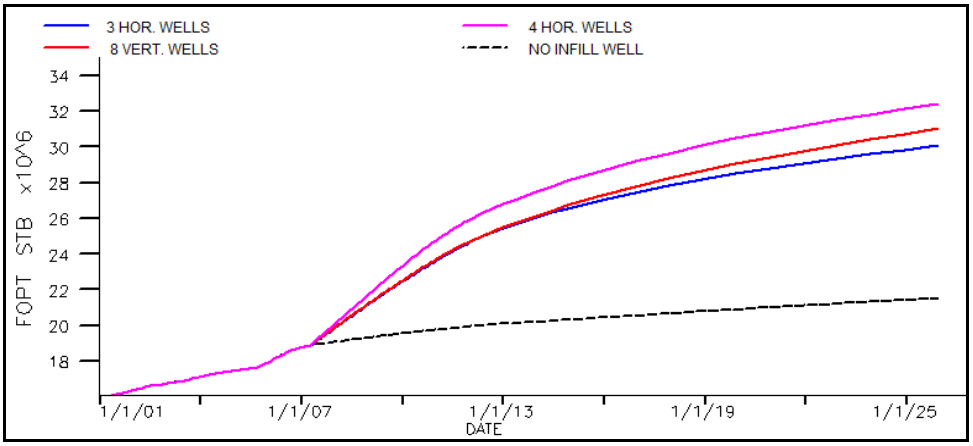

Note: The dotted line represent the do nothing case.

5 Screening using experimental design

Table 2 shows uncertain parameters and their ranges in terms of multiplier on the base case model. The description of the different parameters is given in the Nomenclature. Using the parameters in Table 2, a Placket-Burman design was conducted. The design matrix is shown in Table 3. The '+1' and '–1' correspond to the absolute high and low values of the variables. The simulation was done on the forecast reserves and response value was recorded for 18 years of forecast. With the analysis of variance (ANOVA), the main effects were computed. The relative contribution of different main factors is presented as Pareto charts in Figure 4. The 'heavy-hitters' identified are: critical water saturation (SWCR), initial water saturation (SWI), oil viscosity (OVISC), horizontal permeability (PERMX), water relative permeability (KRW), vertical permeability (PERMZ) and critical gas saturation (SGRC) at 95% analysis confidence level.

Table 2 Experimental range in terms of multipliers on the base case uncertain parameters

S/N	*Parameters*	*Keywords*	*Multiplier ranges*		
			Minimum value	*Base case value*	*Maximum value*
1	Oil viscosity	OVISC	0.9	1	1.1
2	Horizontal permeability	PERMX	0.57	1	1.29
3	Vertical permeability	PERMZ	0.5	1	6
4	Porosity	PORO	0.9	1	1.1
5	Critical gas saturation	SGCR	0.5	1	1.5
6	Critical water saturation	SWCR	0.53	1	1.07
7	Fault transmissibility multiplier	MULTFLT	0.5	1	2
8	Water relative permeability	KRW	0.36	1	1.25
9	Initial water saturation	SWI	0.65	1	0.9
10	Aquifer pore volume	AQUIPV	0.85	1	1.35

6 Methodology for model development

6.1 Data collection

The development of ANFIS model can be data driven and so a 3-level experimental design that provides sufficient data within the design space is desirable. Central composite experimental design (CCD) was selected for data sampling. An overall of 145 experiments (Appendix C) were performed considering the full factorial of CCD consisting of 128 cube points, 14 axial points, and three centre points for the seven screened 'heavy-hitters'. Each factor was varied over five levels $\pm\alpha$ (axial points), ±1 (factorial points) and '0' (centre-point). After data quality control, 143 valid experimental points were used after quality checking. The two dataset removed was based on failure to preserve original history match.

Figure 4 Pareto-chart showing contribution of different parameters to cumulative oil production after 18 years of forecast with critical water saturation the most significant and porosity the least at 95% confident level (see online version for colours)

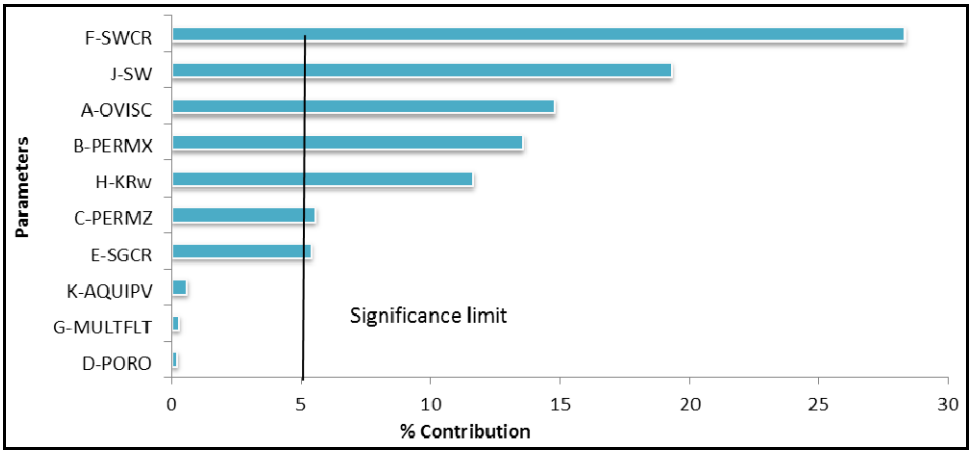

7 Data partitioning

A total of 143 input–output pairs, 72% were randomly selected and were used for training and the remaining 28% of values were used for testing or validation, dictated by the use of triangular membership function. For training, the fuzzy rules were generated directly from the input-output datasets and the model learnt the salient features in the data and automatically adjusted the system parameters to reduce the error between the predicted output and the measured output. The training was achieved using genfis1 and the trainings of these networks were stopped after reaching the minimum error goal of 0.0001 [MATLAB 2007 run on an Intel (R) Core (TM) i5 CPU (2.5 GHz, 6 GB RAM) PC].

8 Optimisation and selection of input parameters

Two optimisation schemes were tested to reveal the inputs that have more percentage impact on the output, an exhaustive and sequential optimisation schemes. Sequential search scheme capable of selecting between one to four input variables from all input candidates and identifies influence of variable and its interactions on model prediction was used. The search began with main factor, two factors interaction, three factors interaction and four factors interaction. Table 4 shows how main factors and their interactions impacted the output for one epoch number using RMSE criteria. The selection of the key factors was based on the magnitude of RMSE of the training and data checking. A low training RMSE and significantly high checking RMSE is a sign of over-fitting. Parameter E (training error of 0.6270 and checking error of 0.7001) is therefore selected first ahead of remaining six main effects. For two interaction factors, EG with lowest training and checking RMSE (0.4774 and 0.5559) was selected. The order of arrangement (EG and not GE) also indicates the degree of significance of the two parameters with E having more impact on the response than G.

Table 3 Placket-Burman design table for ten parameters

f-Run	*A: OVISC*	*B: PERMX*	*C: PERMZ*	*D: PORO*	*E: SGCR*	*F: SWCR*	*G: MULTFLT*	*H: KRW*	*J: SW*	*K: AQUIPV*	*FOPT (stb)*
1	–1	–1	–1	–1	–1	–1	–1	–1	–1	–1	1.99E+07
2	1	–1	–1	–1	1	1	1	–1	1	1	2.05E+07
3	–1	1	–1	–1	–1	1	1	1	–1	1	2.12E+07
4	1	–1	1	1	–1	1	–1	–1	–1	1	2.10E+07
5	–1	–1	1	1	1	–1	1	1	–1	1	1.88E+07
6	1	–1	1	–1	–1	–1	1	1	–1	1	1.98E+07
7	–1	1	1	–1	1	–1	–1	–1	1	1	2.20E+07
8	–1	–1	–1	1	1	1	–1	1	1	–1	2.12E+07
9	–1	1	1	1	–1	1	1	–1	1	–1	2.40E+07
10	1	1	–1	1	–1	–1	–1	1	1	1	2.00E+07
11	1	1	–1	1	1	–1	–1	–1	–1	–1	1.94E+07
12	1	1	1	–1	1	1	1	1	–1	–1	2.04E+07

Table 4 SEQSRCH results of 'heavy-hitters' selection used for proposed model development

Uncertainty	*RMSE*	
	Training	*Testing*
A	0.8020	0.8397
B	0.8631	0.8514
C	0.8638	0.8348
D	0.7554	0.7471
E	0.6270	0.7001
F	0.8237	0.8552
G	0.7642	0.7407
(EA)	0.5533	0.6571
(EB)	0.534	0.6318
(EC)	0.5058	0.6121
(ED)	0.5333	0.6399
(EF)	0.5528	0.6838
(EG)	0.4774	0.5559
(EGA)	0.3264	0.6446
(EGB)	0.3719	0.5642
(EGC)	0.3082	0.514
(EGD	0.3726	0.7366
(EGF)	0.3783	0.7315
(CEGA)	0.0682	0.9566
(CEGB)	0.1344	1.5383
(CEGD)	0.0998	1.5102
(CEGF)	0.1639	1.4011

The selection process is similar for the other higher combination of variables. Three factors searching revealed EGC as having the closest and lowest RMSE (0.3082 and 0.5140) values for training and checking errors. CEGA was selected on searching for four factors with RMSE (0.0682 and 0.9566) for the training and checking errors respectively.

9 Network architecture for ANFIS model

This study utilised MATLAB software to construct the model. The ANFIS network was trained employing grid partitioning to generate FIS. FIS utilises different membership functions. The membership function assigned to each input was tuned using *hybrid* optimisation method (which is a combination of least squares method and gradient steepest descent method) for the parameters associated with the input membership function and the least squares estimation for the parameters associated with the output membership functions. A gradient vector was used to measure how well the fuzzy system is modelling the input-output data. The FIS generated is shown in Figure 5.

Figure 5 consists of three different parts: fuzzifiers, which map the crisp values of the preprocessed input of the model into suitable fuzzy sets represented by membership functions; followed by the inference mechanism or inference engine, which is the computational method to compute the extent to which each rule fires for a given fuzzified input pattern according to an active inference rule; and the last part is a defuzzifier, which maps the crisp values of the preprocessed input of the model into suitable fuzzy sets represented by membership functions and postprocessed to give the output of the fuzzy system based on the crisp signal obtained after defuzzification.

Figure 5 High-level display of fuzzy inference system comprises of fuzzifier for mapping of preprocessed input parameters, inference engine where computation occurs based on input pattern and defuzzifier for output postprocessing (see online version for colours)

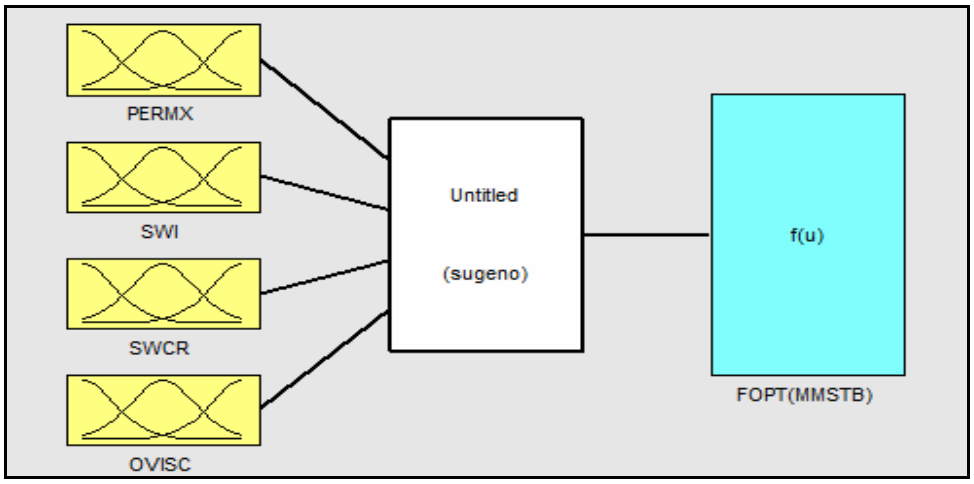

Figure 6 Schematic of ANFIS network consists of four input nodes, eight input membership function nodes, one node for normalised rules, one output membership node, and one output node (see online version for colours)

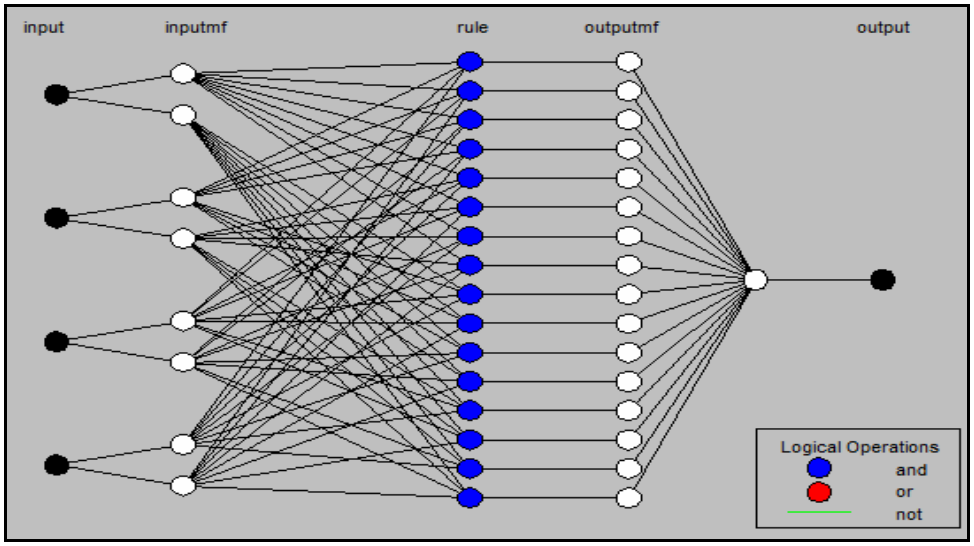

The neuro-fuzzy structure is shown in Figure 6, which consists of four input nodes, eight input membership function nodes, one node for normalised rules, one output membership node, and one output node. Figure 7 shows the rule for four-input FIS and the output panel.

Figure 7 Panel for fuzzy inference system showing the rule for four input FIS and the output panel (see online version for colours)

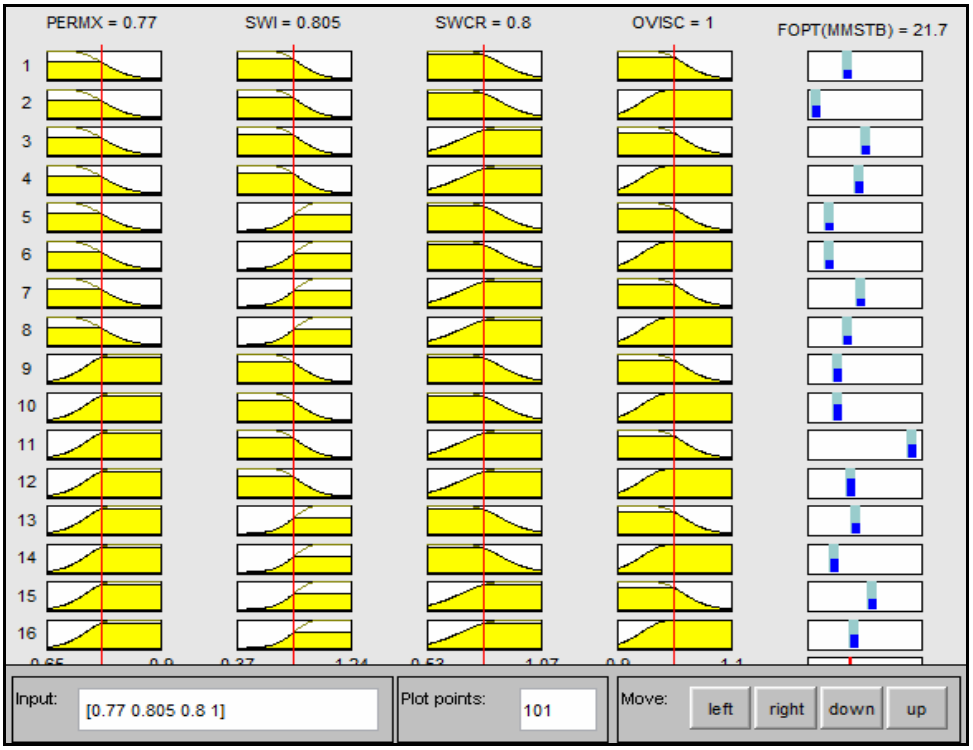

10 Results and discussion

10.1 Influence of membership function

Table 5 shows the different membership functions tested during modelling and how they influence the training and checking errors. Gaussian membership function (Gaussmf) exhibited least over-fitting with R-square value of 96%. It is evident from Figure 8 that as the training error decreased from 0.264917 to 0.22372, the checking error reduced up to epoch number of about 18 and shoot up gently indicating occurrence of minimum over-fitting before it stabilised. Over-fitting was checked by selecting appropriate membership function that associated with the minimum checking error.

Table 5 Influence of different membership function

MF	*RMSE error*		*R-square value*
	Training	*Checking*	
Gbell	0.215383	0.324773	0.95471
Gauss	0.22372	0.304382	0.956
Gauss2	0.21318	0.323268	0.95545
Tri	0.221813	0.302415	0.95673
Pi	0.198293	0.350266	0.95415
Psig	0.223396	0.353501	0.9486
dsig	0.223396	0.353501	0.9486

Figure 8 Error propagation for checking (upper) and training (lower)

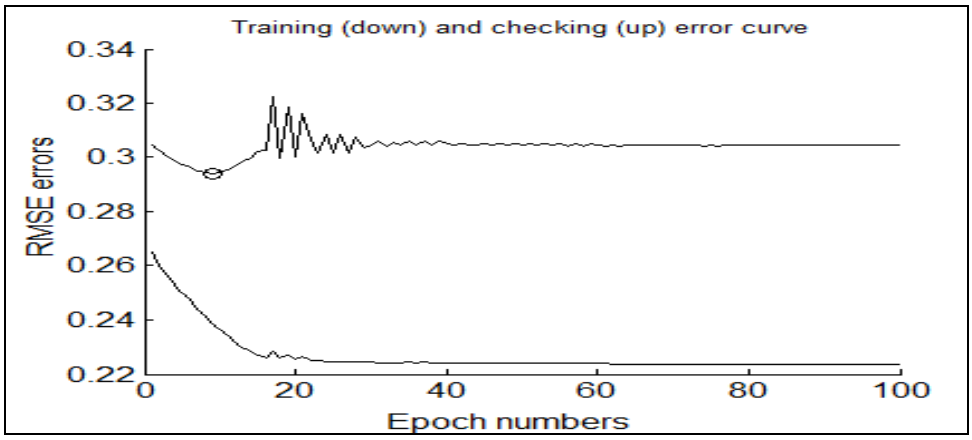

Note: Checking error indicated occurrence of minimum over-fitting at epoch of 18 before it stabilised.

Figure 9 Parity plot of actual and predicted values in ANFIS for training datasets (see online version for colours)

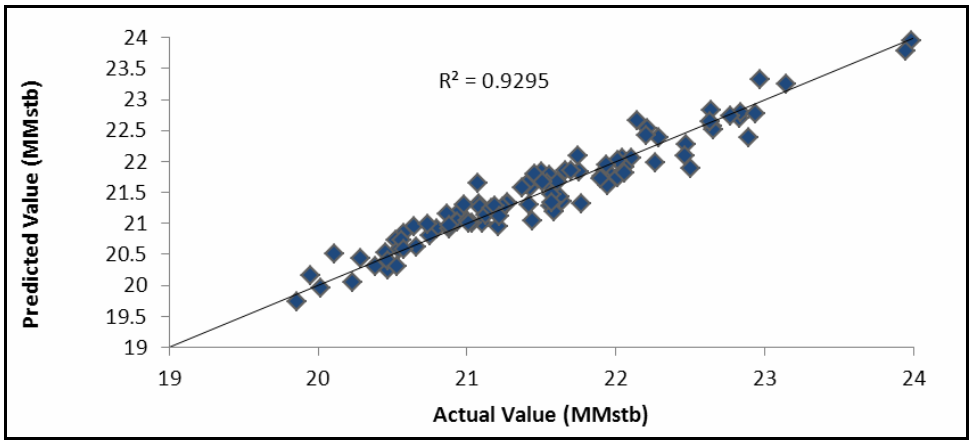

Figure 9 is the cross plot of the trained 100 dataset versus model prediction for the first 100 epoch number. The model intersected most of the data point with correlation coefficient of 93%. Figure 10 depicts the cross plot for the checking data versus model prediction for the remaining 43 dataset. The prediction coefficient is 0.8455 and the root mean square error is 4%.

Figure 11 shows the parity plot of actual reserves value versus ANFIS prediction for the whole dataset used. The correlation coefficient of 95.6% is more than desired and indicates that the model is predictive.

Figure 10 Parity plot of actual and predicted values in ANFIS for checking datasets (see online version for colours)

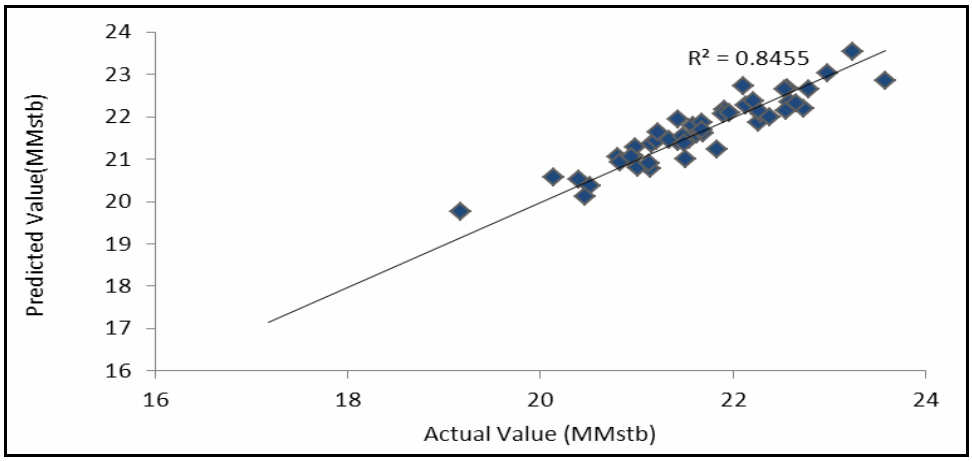

Figure 11 Parity plot of actual and predicted values in ANFIS for all datasets (see online version for colours)

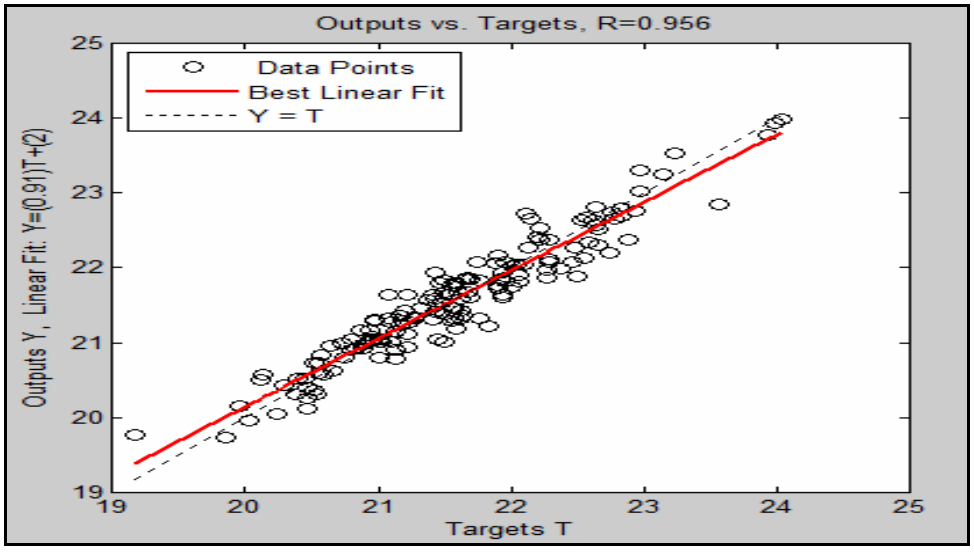

11 Summary

1 Investment in E&P projects are based on forecast quantities. Reservoir simulation is often performed to access and evaluate different development concepts in this case an infill drilling. The decision to invest is always hinged on the result from production forecast the realistic value of which is difficult to achieve. This study developed a predictive model for production forecast after drilling new horizontal wells.

2 Experimental design and numerical simulation were integrated to develop ANFIS based proxy model for the production forecast.

3 Experimental design was used in this study to serve dual purposes: uncertainty screening and data gathering when combined with numerical simulation.

4 Finally, response surface was developed by performing ANOVA on the experimental data generated and compared its performance using average absolute percentage relative error (AAPRE). The detail of the ANOVA is given in Appendix A.

12 Conclusions

A model for the prediction of production forecast was developed by integrating experimental design and adaptive neuro-fuzzy network and the following conclusions were made:

1 the prediction from the model gives a better prediction and accuracy (AAPRE of 0.7406 and R-square of 0.956) than the RSM (AAPRE of 2.913 and 0.8819) usually developed from the analysis of experimental design

2 ANFIS model utilised fewer parameters when compare with RSM-based proxy-model and therefore offers more flexibility where data availability poses serious challenge.

Competing interest

The authors declare that there is no conflict of interests regarding the publication of this paper.

Acknowledgements

The authors acknowledged Schlumberger for providing the software at AUST for simulation. We also wish to acknowledge Petroleum Technology Development Fund (PTDF) for supporting this research.

References

Badru, O. and Kabir, S. (2003) 'Well placement optimization in field development', Paper SPE 84191 presented at the *SPE Annual Technical Conference and Exhibition*, Denver, Colorado, 5–8 October.

Cullick, A.S., Johnson, D. and Shi, G. (2006) 'Improved and more-rapid history matching with a nonlinear proxy and global optimization', Paper SPE 101993 presented at the *SPE Annual Technical Conference and Exhibition*, San Antonio, Texas, 24–27 September.

Fishman, G.S. (1996) *Monte Carlo: Concepts, Algorithms and Applications*, Springer-Verlag, New York.

Guyagular, B., Horne, R.N., Rogers, L. and Rosenzweig, J.J. (2000) 'Optimization of well placement in a Gulf of Mexico waterflooding project', Paper SPE 63221 presented at the *SPE Annual Technical Conference and Exhibition*, Dallas, Texas, 1–4 October.

Jang, J-S.R. (1993) 'ANFIS: adaptive-network-based fuzzy inference system', *Transactions on Systems, Man, and Cybernetics*, Vol. 23, No. 3, pp665–685.

Mohaghegh, S. (2000) 'Virtual-intelligence applications in petroleum engineering: Part 1 – artificial neural networks', *Journal of Petroleum Technology*, September, Vol. 52, No. 9, p.8.

Olatunji, S.O., Selamat, A., Abdul Raheem, A. and Omatu, S. (2011) 'Modeling the correlations of crude oil properties based on sensitivity based linear learning method', *Engineering Applications of Artificial Intelligence*, Vol. 24, No. 4, pp.686–696.

Ozdogan, U., Sahni, A., Yeten, B., Guyagular, B. and Chen, W.H. (2005) 'Efficient assessment and optimization of a deepwater asset development using fixed pattern approach', Paper SPE 95792 presented at the *SPE Annual Technical Conference and Exhibition*, Dallas, Texas, 10–12 October.

Peng, C.Y. and Gupta, R. (2004) *Experimental Design and Analyses Methods on Multiple Deterministic Modeling for Quantifying Integrated Modeling and for Asset Management*, Kuala Lumpur, Malaysia, 29–30 March.

Rwechungura, R., Dadashpour, M. and Kleppe, J. (2011) 'Advanced history matching techniques reviewed', SPE 142497 presented at the *SPE Middle East Oil and Gas Show and Conference*, Manama, Bahrain, 6–9 March.

Salam, K.K., Araromi, D.O. and Ikiensikimama, S.S. (2011) 'Neuro-fuzzy modeling for the prediction of below-bubble-point viscosity', *Petroleum Science and Technology*, Vol. 29, No. 17, pp.1741–1752.

Sampaio, T.P., Ferreira Filho, V.J.M. and de Sa Neto, A. (2009) SPE 122148 presented at the *SPE Latin American and Caribbean Petroleum Engineering Conference*, Cartagena, Colombia, 31 May–3 June.

Yeten, B. (2007) 'Optimization of field development', *Proceedings of 9th international Forum on Reservoir Simulation*, Abu Dhabi, UAE, 9–13 December.

Yeten, B., Castellini, A., Guyagular, B. and Chen, W.H. (2005) 'A comparison study on experimental design and response surface methodologies', Paper SPE 93347 presented at the *SPE Reservoir Simulation Symposium*, Houston, Texas, USA, January 31–February 2.

Appendix A

Response surface modelling using central composite design

Table A1 comprises of the list of all the 'heavy-hitters' and their range used for uncertainty analysis. Model selection was based on the sequential model sum of squares and also on model statistics. From the ANOVA, Tables A2 and A3, it is evident that factorial model was suitable with F value of 2.54 and p value less than the threshold 0.005. The model (Linear+2FI) if selected have 0.1% that it occurs due to noise. The values of R-square including adjusted and predicted also attest to this conclusion with 91, 89 and 86% coefficients.

Table A1 Experimental range in terms of multipliers on the base case uncertain parameters

S/N	*Parameters*	*Keywords*	*Multiplier ranges*		
			Minimum value	*Base case value*	*Maximum value*
1	Oil viscosity	OVISC	0.9	1	1.1
2	Horizontal permeability	PERMX	0.57	1	1.29
3	Vertical permeability	PERMZ	0.5	1	6
4	Critical gas saturation	SGCR	0.5	1	1.5
5	Critical water saturation	SWCR	0.53	1	1.07
6	Water relative permeability	KRW	0.36	1	1.25
7	Initial water saturation	SWI	0.65	1	0.9

Table A2 Sequential model sum of squares

	Sum of source	*DF*	*Mean squares*	*F-value*	*Prob > F*
Mean	63,979.36	1	63,979.36		
Linear	339.15	7	48.45	121.66	< 0.0001
2FI	16.82	21	0.8	2.51	0.0011
Quadratic	2.07	7	0.3	0.92	0.4932
Cubic	15.93	41	0.39	1.42	0.108
Residual	16.16	59	0.27		
Total	64,369.49	136	473.31		

Table A3 Model summary statistics

Source	*Std. dev.*	*R-squared*	*Adjusted R-squared*	*Predicted R-squared*	*PRESS*
Linear	0.63	0.8693	0.8622	0.8517	57.87
2FI	0.56	0.9125	0.8895	0.8627	53.57
Quadratic	0.57	0.9178	0.889	0.8034	76.7
Cubic	0.52	0.9586	0.9052	+	Aliased

The model regressor were selected based on the ANOVA of individual model coefficients using value of 'Prob > F' statistics. The result obtained from the ANOVA is presented in Table A4. According to Table A4, the Model F-value of 95.28 implies the model is significant which means that there is only a 0.01% chance that a 'Model F-Value' this large could occur due to noise. It was observed that the probability coefficients (p-value) for A-PERMX, B-PERMZ, C-SWI, D-KRW, E-SWCR, F-SGCR, G-OVISC, AF, CG, DE and DG were less than 0.05, given a certainty level of 95% showing that the selected model parameters were significant.

The final response surface equation is:

$$\begin{aligned} FOPT = {} & a_0 + a_1 PERMX + a_2 PERMZ + a_3 SWI + a_4 KRW + a_5 SWCR \\ & + a_6 SGCR + a_7 OVISC + a_8 PERMX * SGCR + a_9 SWI * OVISC \\ & + a_{10} KRW * SWCR + a_{10} KRW * OVISC \end{aligned} \tag{A1}$$

Coefficient of response surface in the equation											
a0	*a1*	*a2*	*a3*	*a4*	*a5*	*a6*	*a7*	*a8*	*a9*	*a10*	*a11*
14.93	0.275	0.1	17.76	–3.018	5.012	–1.074	–0.773	0.661	–12.62	–1.227	3.279

Figure A1 is the cross plot of the model prediction versus actual experimental values. The degree to which the data points align to X = Y line determine how predictive the model is. The coefficient of correlation (R-square = 88%) shows the model is predictive to acceptable margin of error.

Table A4 ANOVA for response surface reduced 2FI model

Source	*Sum of squares*	*DF*	*Mean square*	*F-value*	*Prob > F*	
Model	348.86	11	31.71	95.28	< 0.0001	Significant
A-PERMX	16.48	1	16.48	49.53	< 0.0001	
B-PERMZ	7.42	1	7.42	22.3	< 0.0001	
C-SW	55.11	1	55.11	165.57	< 0.0001	
D-KRW	14.93	1	14.93	44.86	< 0.0001	
E-SWCR	157.47	1	157.47	473.08	< 0.0001	
F-SGCR	7.66	1	7.66	23.02	< 0.0001	
G-OVISC	91	1	91	273.39	< 0.0001	
AF	1.73	1	1.73	5.2	0.0244	
CG	3.06	1	3.06	9.18	0.003	
DE	2.67	1	2.67	8.01	0.0054	
DG	2.61	1	2.61	7.85	0.0059	
Residual	41.27	124	0.33			
Cor Total	390.13	135				

Figure A1 Parity plot of actual and predicted values for response surface from CCD (see online version for colours)

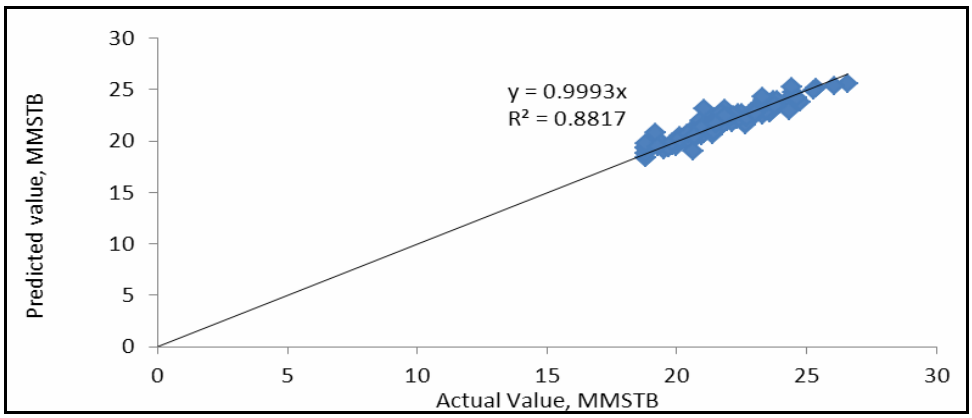

Appendix B

Property histograms showing variation of different reservoir sub-region in terms of porosity and permeability distributions.

Figure B1 Permeability Histograms for all the reservoir sub-regions (see online version for colours)

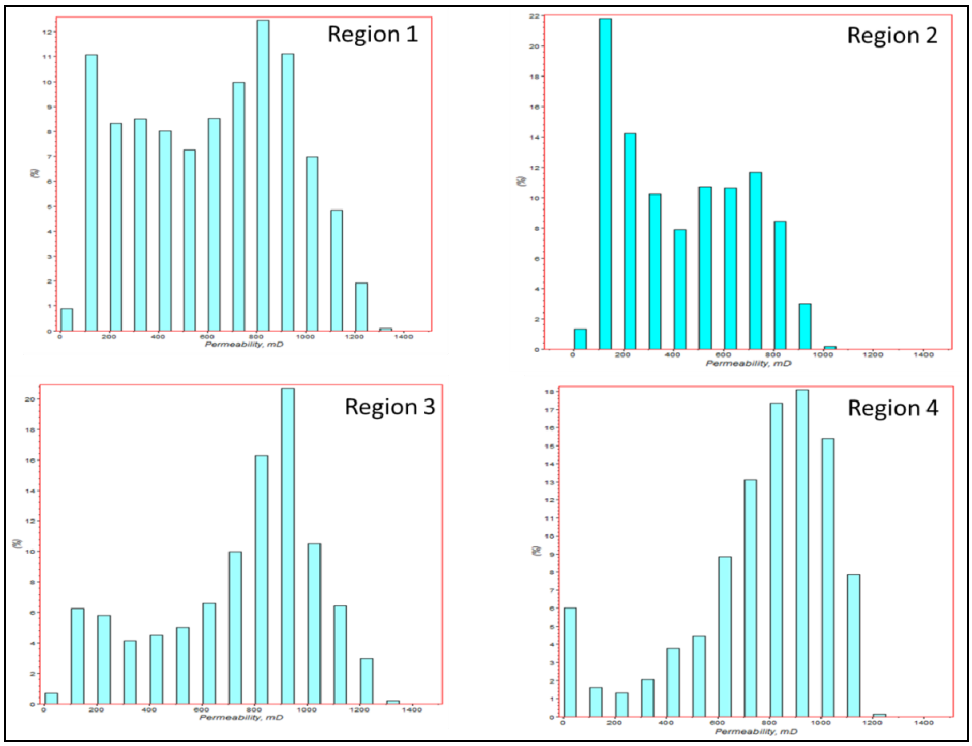

Figure B2 Porosity histograms for all the reservoir sub-regions (see online version for colours)

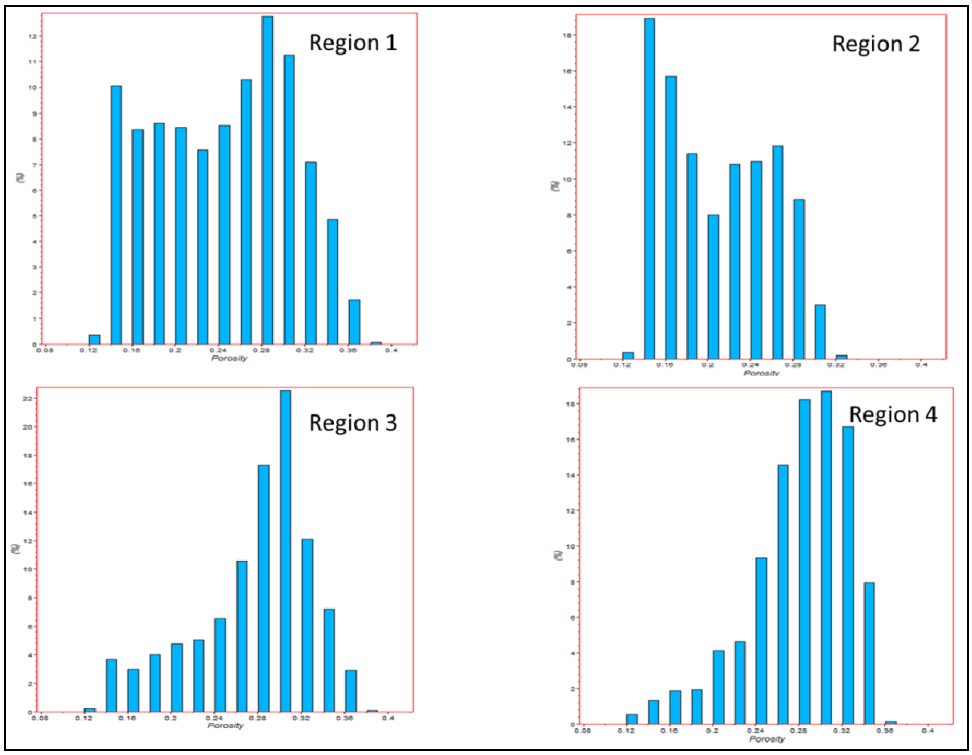

Appendix C

Table C1 Data collected using the CCD

Run	*A: PERMX*	*B: PERMZ*	*C: SW*	*D: KRW@S*	*E: SWCR*	*F: SGCR*	*G: OVSC*	*FOPT (MMstb)*
1	0.57	0.5	0.9	1.25	0.53	1.5	1.1	18.8122
2	1.29	0.5	0.65	0.36	0.53	1.5	1.1	18.8157
3	0.57	5	0.9	0.36	1.07	0.5	1.1	23.1352
4	1.29	5	0.9	1.25	0.53	1.5	0.9	22.0524
5	0.57	0.5	0.65	1.25	0.53	1.5	0.9	18.8203
6	1.29	5	0.65	0.36	1.07	1.5	1.1	22.3992
7	0.57	0.5	0.65	1.25	1.07	1.5	0.9	21.6266
8	1.29	0.5	0.9	0.36	0.53	1.5	1.1	20.3431
9	1.29	5	0.65	1.25	1.07	1.5	1.1	21.4155
10	2.14	2.75	0.78	0.8	0.8	1	1	21.7073
11	0.57	0.5	0.65	0.36	1.07	1.5	0.9	22.2557
12	1.29	5	0.65	1.25	0.53	1.5	0.9	25.2557
13	0.57	0.5	0.65	1.25	0.53	0.5	0.9	20.1382
14	0.57	0.5	0.65	0.36	0.53	0.5	1.1	19.5311
15	0.57	0.5	0.65	0.36	1.07	0.5	1.1	21.0733
16	1.29	0.5	0.65	0.36	1.07	1.5	1.1	22.1336
17	0.57	5	0.9	1.25	1.07	0.5	0.9	23.8764
18	1.29	5	0.65	0.36	1.07	1.5	0.9	24.7510
19	1.29	0.5	0.9	0.36	0.53	1.5	0.9	23.3246
20	0.93	2.75	0.78	2.3	0.8	1	1	21.3688
21	1.29	5	0.9	0.36	0.53	0.5	1.1	20.5187
22	0.57	0.5	0.9	0.36	0.53	0.5	1.1	20.3436
23	1.29	5	0.9	1.25	1.07	1.5	0.9	24.6412
24	0.93	–4.83	0.78	0.8	0.8	1	1	21.4119

Table C1 Data collected using the CCD (continued)

Run	*A: PERMX*	*B: PERMZ*	*C: SW*	*D: KRW@S*	*E: SWCR*	*F: SGCR*	*G: OVSC*	*FOPT (MMstb)*
25	1.29	0.5	0.65	0.36	1.07	0.5	0.9	24.1527
26	1.29	0.5	0.9	0.36	0.53	0.5	1.1	20.6541
27	0.93	2.75	0.78	–0.68	0.8	1	1	23.0267
28	0.93	2.75	0.78	0.8	0.8	–0.68	1	21.8378
29	1.29	0.5	0.9	1.25	0.53	0.5	0.9	22.1298
30	0.57	5	0.65	1.25	1.07	0.5	0.9	22.6888
31	0.57	5	0.65	0.36	1.07	1.5	1.1	21.3166
32	0.57	5	0.9	1.25	1.07	1.5	1.1	21.8120
33	0.57	0.5	0.9	0.36	0.53	1.5	0.9	22.6442
34	0.93	2.75	1.2	0.8	0.8	1	1	24.0267
35	1.29	5	0.9	0.36	0.53	0.5	0.9	21.8569
36	1.29	5	0.65	1.25	0.53	0.5	0.9	21.4757
37	0.93	2.75	0.78	0.8	0.8	1	1	21.5352
38	1.29	5	0.65	1.25	1.07	0.5	0.9	23.5770
39	0.57	0.5	0.9	0.36	0.53	1.5	1.1	19.7099
40	1.29	5	0.9	1.25	0.53	0.5	1.1	21.1066
41	1.29	0.5	0.9	1.25	1.07	1.5	1.1	21.9070
42	1.29	5	0.65	0.36	0.53	1.5	0.9	20.7368
43	0.93	2.75	0.78	0.8	–0.11	1	1	19.0473
44	0.57	0.5	0.9	1.25	1.07	0.5	1.1	21.4696
45	0.57	0.5	0.65	1.25	1.07	0.5	1.1	20.7338
46	1.29	0.5	0.65	0.36	0.53	1.5	0.9	20.6415
47	1.29	0.5	0.65	0.36	0.53	0.5	1.1	19.8321
48	0.57	0.5	0.65	1.25	1.07	0.5	0.9	21.9283

Table C1 Data collected using the CCD (continued)

Run	*A: PERMX*	*B: PERMZ*	*C: SW*	*D: KRW@S*	*E: SWCR*	*F: SGCR*	*G: OVSC*	*FOPT (MMstb)*
49	0.57	5	0.9	0.36	0.53	1.5	1.1	19.8473
50	–0.28	2.75	0.78	0.8	0.8	1	1	20.6670
51	0.57	5	0.65	1.25	1.07	1.5	0.9	22.6415
52	1.29	0.5	0.65	1.25	0.53	0.5	0.9	20.9744
53	1.29	5	0.65	1.25	0.53	0.5	1.1	20.3529
54	0.57	0.5	0.9	0.36	0.53	0.5	0.9	21.3190
55	1.29	0.5	0.9	1.25	0.53	0.5	1.1	20.7658
56	1.29	5	0.78	0.36	0.53	0.5	1.1	20.3391
57	1.29	0.5	0.65	1.25	1.07	1.5	0.9	22.3350
58	1.29	5	0.9	0.36	1.07	1.5	0.9	26.0848
59	1.29	5	0.9	1.25	1.07	0.5	1.1	22.5086
60	0.93	2.75	0.78	0.8	0.8	1	0.66	23.3181
61	0.57	5	0.65	0.36	0.53	0.5	0.9	20.7989
62	0.57	0.5	0.9	0.36	1.07	0.5	0.9	24.4832
63	0.57	5	0.9	0.36	0.53	1.5	0.9	20.9042
64	0.57	0.5	0.9	1.25	0.53	1.5	0.9	20.5857
65	1.29	5	0.65	0.36	0.53	1.5	1.1	19.4279
66	0.57	5	0.65	1.25	0.53	1.5	1.1	18.8040
67	0.57	5	0.9	1.25	0.53	0.5	0.9	22.4900
68	0.57	5	0.9	0.36	0.53	0.5	1.1	20.6541
69	0.57	5	0.9	0.36	1.07	1.5	1.1	22.6961
70	0.57	5	0.9	1.25	0.53	0.5	1.1	20.6307
71	0.57	5	0.65	1.25	0.53	0.5	0.9	20.1382
72	0.57	5	0.65	1.25	0.53	1.5	0.9	18.8273

Table C1 Data collected using the CCD (continued)

Run	*A: PERMX*	*B: PERMZ*	*C: SW*	*D: KRW@S*	*E: SWCR*	*F: SGCR*	*G: OVSC*	*FOPT (MMstb)*
73	1.29	0.5	0.9	1.25	0.53	1.5	1.1	20.4642
74	0.57	5	0.65	1.25	1.07	1.5	1.1	20.4327
75	0.57	0.5	0.9	0.36	1.07	0.5	1.1	22.5010
76	1.29	5	0.9	0.36	1.07	0.5	0.9	26.5719
77	1.29	0.5	0.9	0.36	1.07	1.5	1.1	23.0481
78	1.29	5	0.9	0.36	1.07	0.5	1.1	23.7883
79	0.57	0.5	0.65	1.25	0.53	0.5	1.1	25.5719
80	0.57	5	0.9	1.25	1.07	0.5	1.1	22.0995
81	0.57	0.5	0.9	1.25	1.07	1.5	1.1	20.9552
82	1.29	0.5	0.65	1.25	0.53	1.5	0.9	19.2610
83	0.57	0.5	0.9	1.25	0.53	0.5	1.1	20.0550
84	0.57	0.5	0.65	0.36	1.07	0.5	0.9	23.0715
85	1.29	0.5	0.65	1.25	0.53	0.5	1.1	19.6872
86	0.57	0.5	0.9	1.25	1.07	1.5	0.9	22.9086
87	0.57	5	0.9	1.25	0.53	1.5	0.9	21.1922
88	0.57	0.5	0.65	1.25	1.07	1.5	1.1	20.1214
89	0.57	0.5	0.65	1.25	0.53	1.5	1	18.7978
90	1.29	5	0.9	0.36	1.07	1.5	1.1	21.0455
91	1.29	5	0.65	0.36	0.53	0.5	0.9	20.9744
92	0.57	0.5	0.9	1.25	1.07	0.5	0.9	23.1701
93	0.57	0.5	0.9	0.36	1.07	1.5	1.1	21.7174
94	1.29	0.5	0.9	1.25	1.07	1.5	0.9	23.5204
95	1.29	5	0.65	1.25	1.07	1.5	0.9	23.0475
96	1.29	5	0.9	1.25	1.07	1.5	1.1	22.1630

Table C1 Data collected using the CCD (continued)

Run	*A: PERMX*	*B: PERMZ*	*C: SW*	*D: KRW@S*	*E: SWCR*	*F: SGCR*	*G: OVSC*	*FOPT (MMstb)*
97	0.57	5	0.65	0.36	0.53	0.5	1.1	23.1204
98	0.57	0.5	0.9	1.25	0.53	0.5	0.9	21.6179
99	0.57	5	0.65	0.36	1.07	0.5	1.1	21.9125
100	1.29	0.5	0.9	0.36	0.53	0.5	0.9	22.3575
101	0.57	5	0.65	1.25	1.07	0.5	1.1	21.0749
102	1.29	5	0.9	0.36	0.53	1.5	1.1	20.3764
103	0.93	2.75	0.78	0.8	0.8	1	1.34	20.6197
104	0.93	10.32	0.78	0.8	0.8	1	1	21.9389
105	0.57	5	0.9	0.36	1.07	0.5	0.9	25.3627
106	1.29	5	0.65	0.36	1.07	0.5	1.1	22.6530
107	0.57	5	0.65	0.36	1.07	1.5	0.9	23.6267
108	1.29	0.5	0.65	1.25	0.53	1.5	1.1	24.6016
109	1.29	0.5	0.9	0.36	1.07	0.5	0.9	25.3684
110	0.57	5	0.65	0.36	1.07	0.5	0.9	23.8358
111	1.29	5	0.65	1.25	0.53	1.5	1.1	19.1139
112	1.29	5	0.9	1.25	0.53	1.5	1.1	21.0455
113	1.29	5	0.9	0.36	0.53	1.5	0.9	24.3291
114	0.57	5	0.65	0.36	0.53	1.5	0.9	20.5364
115	0.57	5	0.65	1.25	0.53	0.5	1.1	19.9665
116	1.29	0.5	0.65	1.25	1.07	0.5	1.1	21.2923
117	1.29	5	0.9	1.25	1.07	0.5	0.9	24.5016
118	1.29	0.5	0.9	0.36	1.07	0.5	1.1	23.4522
119	0.57	0.5	0.65	0.36	0.53	1.5	0.9	19.9409
120	1.29	0.5	0.9	1.25	1.07	0.5	0.9	23.8764

Table C1 Data collected using the CCD (continued)

Run	*A: PERMX*	*B: PERMZ*	*C: SW*	*D: KRW@S*	*E: SWCR*	*F: SGCR*	*G: OVSC*	*FOPT (MMstb)*
121	0.57	0.5	0.65	0.36	1.07	1.5	1.1	19.1637
122	0.57	5	0.9	0.36	1.07	1.5	0.9	21.3127
123	1.29	0.5	0.9	1.25	1.07	0.5	1.1	21.8837
124	1.29	0.5	0.65	0.36	1.07	1.5	0.9	23.5699
125	1.29	0.5	0.65	1.25	1.07	1.5	1.1	20.9733
126	0.57	0.5	0.65	0.36	0.53	1.5	1.1	18.8003
127	0.93	2.75	0.78	0.8	0.8	2.68	1	21.4367
128	0.57	5	0.9	1.25	0.53	1.5	1.1	18.8205
129	1.29	5	0.65	1.25	1.07	0.5	1.1	21.4313
130	1.29	0.5	0.65	0.36	1.07	0.5	1.1	21.4347
131	1.29	0.5	0.65	0.36	0.53	0.5	0.9	20.9266
132	1.29	5	0.9	1.25	0.53	0.5	0.9	22.3127
133	1.29	5	0.65	0.36	1.07	0.5	0.9	23.3554
134	0.57	5	0.9	1.25	1.07	1.5	0.9	23.6727
135	0.57	0.5	0.9	0.36	1.07	1.5	0.9	23.3554
136	0.93	2.75	0.78	0.8	1.71	1	1	24.421
137	0.57	0.5	0.65	0.36	0.53	0.5	0.9	20.5845
138	0.57	5	0.9	0.36	0.53	0.5	0.9	23.5896
139	1.29	0.5	0.9	1.25	0.53	1.5	0.9	21.6737
140	1.29	0.5	0.9	0.36	1.07	1.5	0.9	25.2784
141	0.93	2.75	0.35	0.8	0.8	1	1	19.2872
142	0.57	5	0.65	0.36	0.53	1.5	1.1	18.8071
143	1.29	0.5	0.65	1.25	1.07	0.5	0.9	22.3605

Appendix D

Model program/data: integrating both static and dynamic properties (see online version for colours)

```
RUNSPEC

TITLE
--SIMULATION DATA FILE

FIELD

OIL
GAS
WATER
DISGAS

SAVE
/

MEMORY
 620 620 /

DIMENS
55  140  25 /

EQLDIMS
--nregs  #d Pnodes  #d RVnodes
   3  1000000 4*  /

FAULTDIM
  150 /

ENDSCALE
 'NODIR'     'REVERS'        /

TABDIMS
--ntsfun ntpvt nssfun nppvt ntfip nrpvt nrpvt ntendp   pmaint
   3     3      50    50    2    50    50    1    /

REGDIMS
--ntfip  #sets
   3    1  3*       /

WELLDIMS
--maxw conW grup wlG stg strm
   100   100   100   100 /

ACTDIMS
   10   2*   /

NSTACK
 75  /

UNIFIN
UNIFOUT

--NOSIM

START
 1 'FEB' 1971 /

------------------------------------------------------------------------
```

```
GRID
--------------------------------------------------------------------------
INIT
--
NOECHO
--
--
GRIDFILE
 2 2 /

INCLUDE
GRID.grdecl /

INCLUDE
PORO.grdecl /

INCLUDE
PERM.grdecl /

INCLUDE
FAULTS.grdecl /

MULTIPLY
PERMX 0.33 /
/
MULTIPLY
PERMY 0.33 /
/
MULTIPLY
PERMZ 0.012 /
/

MULTIPLY
PERMY 0.2 8 10 93 96 6 25 /
/
-- modify transmissibility accross a fault

MULTFLT
 'F1_1' 0.099/
'F1_2' 1.98 /
/
NEWTRAN
--------------------------------------------------------------------------
EDIT
--------------------------------------------------------------------------
MULTIPLY
TRANX 0.01 5 28 57 92 9 11 /
/
MULTIPLY
TRANY 0.01 5 28 57 92 9 11 /
/

NOWARN
```

```
PROPS
----------------------------------------------------------------------
INCLUDE
SWL.GRDECL /
/

SWOF
--Sw  Krw Krow  Pcow
0.05  0 0.598 0
0.21976 0.00864 0.20516 0
0.25929 0.02124 0.12236 0
0.31624 0.04032 0.04048 0
0.3752  0.0576  0.0184  0
0.43081 0.0702  0.01472 0
0.85  0.1008  0 0
1 1 0 0
/


SGOF
--#NAME?  Krg Krog  Pcgo
0 0 0.598 0
0.01  0 0.552 0
0.2114912 0.04158 0.2944  0
0.46382208  0.1188  0.1104  0
0.5542528 0.1518  0.06808 0
0.75261696  0.2277  0.0184  0
0.8094755 0.29832 0 0
1   0.63  0 0

/

INCLUDE
Tunned_AK_PVT_PVT.inc /

----------------------------------------------------------------------
REGIONS
----------------------------------------------------------------------
INCLUDE
 Regionsection-NEW.inc /

----------------------------------------------------------------------
SOLUTION
----------------------------------------------------------------------
DATUM
4550 /

EQUIL
-- Equilibration Data Specification - Based on MDT
--    href      pref     woc   pcwoc   hgoc    pcgoc
  4550     1930   4575   0      4444     0      1     1     20  / region 1


RSVD
4000 0.000
/


RPTSOL
  'FIP=2' 'RESTART=1' /

RPTRST
 BASIC=3 FIP=2 /
----------------------------------------------------------------------
```

```
SUMMARY
--------------------------------------------------------------------
RPTONLY
RPTSMRY
   0 /
--SEPARATE
EXCEL
FOE
FPR
FOPR
FOPRH
FGPR
FWPR
FWCT
FWCTH
FGOR
FGORH
FWIT
FWITH
FOPT
FOPTH
FWPT
FWPTH
FVPR
FLPT
FLPTH
FLPR
FGPT
FGPTH
TCPU
/
--------------------------------------------------------------------
SCHEDULE
--------------------------------------------------------------------
SKIPREST
/
MESSAGES
 2* 10000  10000 4*  10000 10000 /

TUNING
 /
 /
 2* 75 / 1* 10 /

WHISTCTL
ORAT /
/

DRSDT
 0.0  /

INCLUDE
SCHEDULE.SCH  /

/
END
```

Terms and nomenclature

ANFIS	Adaptive neuro-fuzzy inference system
M	Thousand
MM	Million
STB	Stock-tank-barrel
MULTFLT	Fault transmissibility multiplier
PV	Pore volume
FVF	Oil formation volume factor
F	Field
WCT	Water cut
OPT	Total oil production
WPT	Total water production
GOR	Gas-oil ratio
PERMX	Horizontal permeability
PERMZ	Vertical permeability
WBT	Water breakthrough time
SWI	Initial water saturation
PORO	Porosity
OVISC	Oil viscosity